THE JOURNAL OF PHYSICAL CHEMISTRY A
LETTERS

2006, *110,* 5967−5972
Published on Web 04/20/2006

Electron Transfer Reactivity in Matrix-Assisted Laser Desorption/Ionization (MALDI): Ionization Energy, Electron Affinity and Performance of the DCTB Matrix within the Thermochemical Framework

Yury V. Vasil'ev,*,†,‡ Olga G. Khvostenko,§ Alexey V. Streletskii,† Olga V. Boltalina,# Sotirios G. Kotsiris,† and Thomas Drewello*,†

[a]Department of Chemistry, University of Warwick, Coventry, CV4 7AL, England, [b]Department of Physics, Bashkir State Agricultural University, Ufa, Russia, [c]Institute of Molecular and Crystal Physics, Ufa Research Center, Russian Academy of Sciences, October prospect 151, Ufa 450075, Russia, and [d]Department of Chemistry, Colorado State University, Fort Collins, Colorado 80523

Received: January 26, 2006; In Final Form: March 27, 2006

DCTB [$(H_3C)_3C$-*p*-Ph-CH═C(CH_3)-*trans*-CH═C$(CN)_2$] has recently advanced to the most promising matrix material for matrix-assisted laser desorption/ionization (MALDI) within material sciences. However, data that would allow the evaluation of the electron-transfer reactivity within a thermochemical framework are sparse. The present study reports the first-time determination of the ionization energy (IE) of DCTB applying photoelectron (PE) spectroscopy. The experimental IE (8.54 ± 0.05 eV) is in excellent agreement with the theoretical value of 8.47 eV, obtained by AM1 calculations. The same level of theory determines the electron affinity (EA) as 2.31 eV. Model analytes of known thermochemistry (phenanthrene [$C_{14}H_{10}$], anthracene [$C_{14}H_{10}$] and fluorofullerene [$C_{60}F_{46/48}$]) are used to bracket the electron-transfer reactivity within DCTB-MALDI. The formation of molecular ions of these analytes either is expected or is beyond the thermochemical accessibility of the DCTB matrix.

Introduction

Matrix-assisted laser desorption/ionization (MALDI) is one of the most successful methods for the analysis of fullerene-based derivatives.[1−13] DCTB (*trans*-2-[3-(4-*tert*-butylphenyl)-2-methyl-2-propenylidene]malononitrile) was first introduced as a suitable MALDI matrix for the analysis of these compounds.[7] Not only is this matrix well-established for this purpose,[8−13] but it also has advanced to a key feature for the improved application of MALDI in other important areas within material sciences.[14,15] DCTB-MALDI has contributed to the development of high-throughput screening in combinatorial polymer research[14] and has replaced the use of previously established protocols for analysis of nonvolatile and thermally labile materials.[15]

For MALDI, the analyte is embedded into a second material, the matrix, which is often present in excess and plays an essential part in the overall process of transforming the solid analyte into a gaseous ion. Upon laser irradiation the light absorbing matrix evaporates into the gas phase, assisting in the desorption of the analyte. Matrix ions are formed in a primary ionization step as the result of direct laser activation.[16] The ion formation of the analyte then takes place in a secondary ionization step, whereby the matrix-derived ions interact with the analyte.[17] Depending on the nature of both these reactants, different types of analyte ions can be formed, predominantly including protonated, deprotonated, metal cationized analytes and/or true molecular ions. A detailed thermochemical description of the partners in these reactions is essential to the understanding of MALDI and thus to the optimization of the method.[16,17]

Compared to other matrix materials, the use of DCTB in MALDI with derivatized fullerenes often leads to only minor analyte fragmentation and to more pronounced analyte ions.[7−13] It was found early on that ion formation with DCTB occurs at lower laser fluences compared to other frequently used matrix materials,[7] which is beneficial to the overall softness of the process. Analyte ions are mostly formed as the true molecular ions in both ion modes.[7−15] DCTB must therefore possess a favorable thermochemistry to undergo electron-transfer reactions with a large variety of compounds.

For the formation of positive analyte ions, the $DCTB^{+\bullet}$ molecular ion may react according to reaction 1. The energy gain upon neutralization of $DCTB^{+\bullet}$ is roughly equal to the ionization energy (IE) of DCTB and must exceed the IE of the analyte (A) for the reaction to proceed.

$$\mathrm{DCTB}^{+\bullet} + \mathrm{A} \rightarrow \mathrm{A}^{+\bullet} + \mathrm{DCTB} \qquad (\mathrm{IE}_{\mathrm{DCTB}} > \mathrm{IE}_{\mathrm{A}}) \quad (1)$$

The energy balance for the formation of negative analyte ions, whereby the analyte abstracts an electron from the $DCTB^{-\bullet}$ anion (reaction 2), affords that the positive electron affinity (EA) of the analyte exceeds the one of DCTB.

$$\mathrm{DCTB}^{-\bullet} + \mathrm{A} \rightarrow \mathrm{A}^{-\bullet} + \mathrm{DCTB} \qquad (\mathrm{EA}_{\mathrm{DCTB}} < \mathrm{EA}_{\mathrm{A}}) \quad (2)$$

---

* To whom correspondence should be addressed. E-mail: Y.V.V., Y.Vasilev@oregonstate.edu; T.D., T.Drewello@warwick.ac.uk.
† University of Warwick.
‡ Bashkir State Agricultural University.
§ Russian Academy of Sciences.
\# Colorado State University.

10.1021/jp060568f CCC: $33.50

The thermochemical properties of DCTB must therefore lie within these boundaries. DCTB may fulfill these requirements even more favorably than other matrix molecules, to show such evidently broad applicability for fullerene-based[7,8,11−13] and other nonbiological compounds.[15] However, the evaluation of the matrix performance is prevented by the lack of thermochemical data of this matrix.

Experimental Section

The He I PE spectrum was recorded using an ES 3201 spectrometer (St. Petersburg, Russia).[18,19] A DCTB sample was placed into a direct insertion probe which was held at 140 °C. In the ionization chamber, the diffusive molecular beam crossed with the photon beam generated by the helium lamp. Electrons resulting from photoionization of DCTB were analyzed by a semispherical electrostatic analyzer and reached a multiplier. Next, enhanced by an amplifier, the signal was stored in a computer. The PE spectrum was calibrated with the $^2P_{1/2}$ and $^2P_{3/2}$ resonance lines of Ar. The energy resolution was 70 meV, measured as full width at the half-maximum (fwhm) and of the Ar ($^2P_{3/2}$) line. Ionization energies were determined with an accuracy of ±50 meV for sharp PE bands and ±100 meV for broad PE bands or shoulders.

For the MALDI experiments with phenanthrene and anthracene: DCTB ($C_{17}H_{18}N_2$, Fluka) and the respective PAH ($C_{14}H_{10}$, Sigma-Aldrich) were dissolved separately in toluene at known concentrations. Solutions were combined to give molar ratios of analyte to matrix (A/M) of 1:1 and/or 1:10. A droplet of the combined solution was deposited on the metallic sample holder and dried before insertion into the mass spectrometer. The DCTB/fluorofullerene (mostly $C_{60}F_{46/48}$, Kaesdorf AG, Germany) target was prepared using a solvent-free sample preparation protocol, mixing analyte and matrix in a molar ratio of 1:1000 in the solid state and attaching the mixture to the target holder using a double sided glue tape. Mass spectra were obtained following N_2 laser activation at 337 nm and were recorded by linear mode time-of-flight mass spectrometry. The phenanthrene experiments were obtained with an Autoflex (Bruker Daltonics, Bremen, Germany) and all other experiments were performed with a Kompact MALDI IV (Kratos Analytical/Shimadzu, Manchester, U.K.). Up to 200 single laser shots were accumulated for each mass spectrum. The molecular anions of $C_{60}F_x^{-\bullet}$ with $x = 46$ and 48 were not observed earlier at A/M of 1:100[11] but were confirmed here at A/M of 1:1000 by high-resolution experiments ($R_{\mathrm{fwhm}} = 20.000$) using an Ultrafex II ToF/ToF mass spectrometer (Bruker Daltonics, Bremen, Germany).

Results and Discussion

The PE spectrum and the structure of DCTB are depicted in Figure 1. The ionization energies of DCTB associated with the PE bands have been marked by vertical bars. For the interpretation of the PE bands, DCTB has been calculated on the semiempirical AM1 level, using the Gaussian 98 program.[20] At this level of theory the adiabatic ionization energy is obtained as $\mathrm{IE_{ad}} = 8.07$ eV and the vertical IE as $\mathrm{IE_{vert}} = 8.47$ eV. The theoretical ionization energies have been obtained in the case of $\mathrm{IE_{ad}}$ as the difference of the total energies of the neutral and the positive ion both taken at their relaxed geometries and in the case of $\mathrm{IE_{vert}}$ as the difference of the total energies of the neutral and the positive ion both taken at the relaxation geometry of the neutral. These values are in excellent agreement with the experimental values that result from the PE spectrum in Figure 1 ($\mathrm{IE_{ad}} = 8.05 \pm 0.05$ eV and $\mathrm{IE_{vert}} = 8.54 \pm 0.05$ eV).

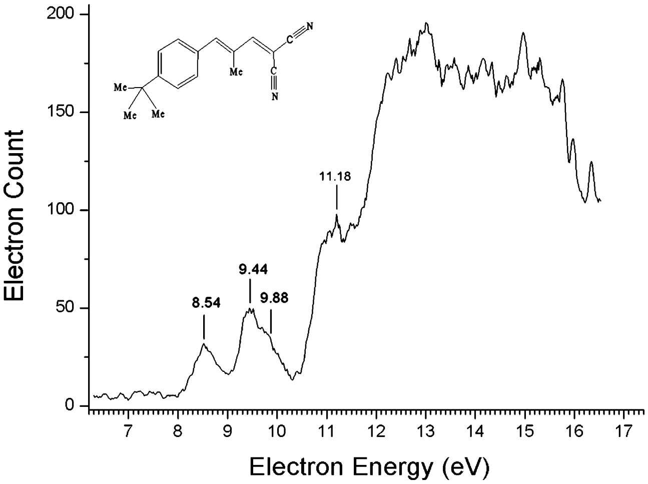

Figure 1. Photoelectron spectrum of DCTB. The vertical bars mark the ionization energies of DCTB associated with the PE bands.

Further interpretation of the PE spectrum through AM1 calculations can be achieved by applying molecular orbital (MO) theory within the framework of Koopmans' theorem. The calculated energies and shapes of the relevant DCTB MOs are shown in Figure 2.

The first PE band at 8.54 eV in Figure 1 can be associated with the $\pi(\tilde{b}_1)-\pi_{\mathrm{CC+CN}}$ highest occupied MO (HOMO) with $\epsilon = -9.124$ eV (Figure 2). This HOMO represents the antibonding combination of the $\pi(\tilde{b}_1)$ MO of benzene and the π-type MO located on the C═C double bonds and the CN groups. The second PE band at 9.44 eV correlates with the noninteracting $\pi(\tilde{a}_2)$ MO on the substituted benzene ring with $\epsilon = -9.924$ eV (HOMO−1 in Figure 2). The $\pi(\tilde{a}_2)$ MO in DCTB is slightly increased in energy with respect to the corresponding MO in unsubstituted benzene, because of the stabilization effect of the electron-withdrawing CN groups. The third PE band at 9.88 eV overlaps with the second band, so that its assignment is rather challenging. However, the AM1 calculations predict a similar close proximity for the energies of HOMO−1 and HOMO−2 (Figure 2). According to the theory, HOMO−2 can be interpreted as the bonding combination of the $\pi(\tilde{b}_1)$ MO on benzene and π_{CC} MO on the double bond adjacent to the benzene ring. Further assignment of the PE bands is not unambiguous because of their strong overlap. The PE band at 11.18 eV may be correlated with the antibonding combination of π MOs located on the CC double bonds and the CN-groups, $\pi_{\mathrm{CC-CN}}$ MO (HOMO−3, Figure 2), which is followed in close energetic succession by two σ-type MOs (HOMO−4 and HOMO−5 in Figure 2). Figure 3 reveals the excellent correlation between theoretical and experimental IEs, resulting in a linear dependence with a correlation coefficient of $R = 0.99897$.

The electron affinity of DCTB has been also calculated as EA = 2.31 eV. The EA was obtained as the difference of the total energies of neutral DCTB and its negative ion, both residing in their ground states following full geometry optimization. The present value is slightly larger than an earlier estimation made on the basis of DFT theory, which resulted in a value of $\mathrm{EA_{DCTB}} = 2.0$ eV.[11] One may expect that the DFT method provides a more reliable value in this type of calculation. However, in the absence of experimental confirmation, $\mathrm{EA_{DCTB}}$ is assumed for the discussion below to lie between 2.0 and 2.3 eV. The negative LUMO energy (Figure 2) also indicates that electron attachment to DCTB is exothermic.

In summary, the thermochemistry of the DCTB matrix would allow the positive-ion MALDI analysis of analytes possessing

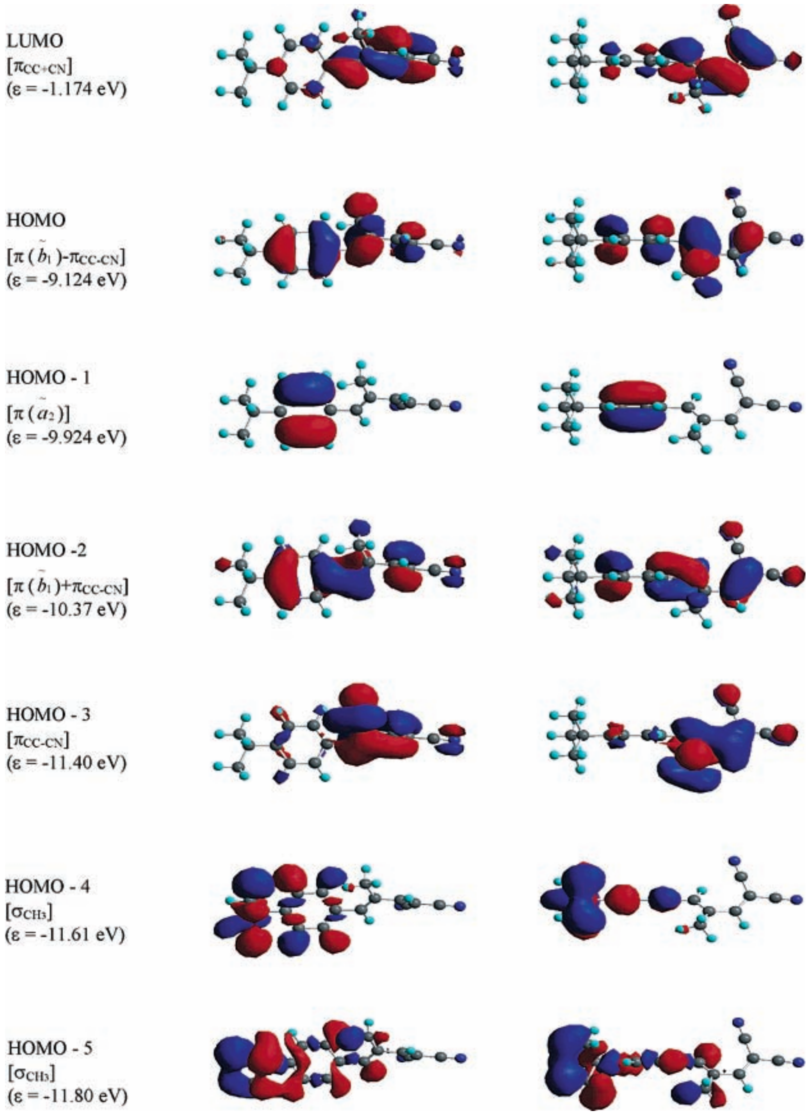

Figure 2. AM1-calculated energies and shapes of the DCTB molecular orbitals.

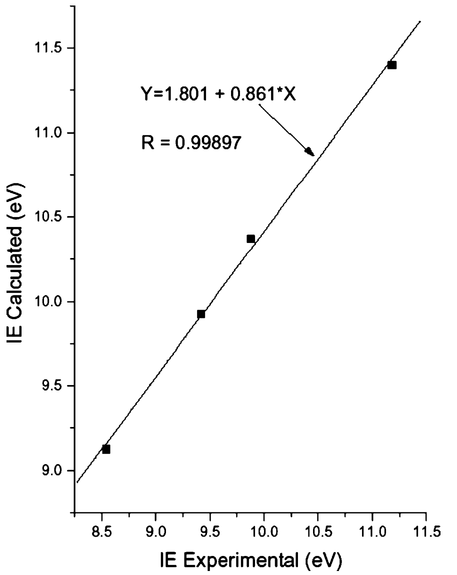

Figure 3. Correlation between theoretical (AM1) and experimental (PE) ionization energies of the DCTB molecule.

IEs below 8.5 eV, whereas negative-ion MALDI would afford analytes with EAs in excess of 2.0−2.3 eV.

First, phenanthrene is studied, as it possesses several features, which make it an interesting model analyte. Phenanthrene shows only poor absorbance of light at the laser wavelength of 337 nm, as indicated by the UV/VIS absorption spectrum (insert Figure 4a, Jinno Laboratory Archive, Japan). Consequently, the molecular ion formation is not resonantly enhanced in direct LDI at 337 nm and in fact only traces at *m*/*z* 178 could be observed occasionally. Figure 4a is a typical example of the positive-ion mass spectrum resulting from direct laser activation (LDI). The molecular ion at *m*/*z* 178 is entirely absent. In Figure 4b,c the positive-ion MALDI mass spectra are depicted, using a phenanthrene:DCTB ratio of 1:1 (Figure 4b) and 1:10 (Figure 4c). The fact that molecular analyte ions are abundantly observed is a striking example of matrix-assisted desorption of a nonabsorbing analyte, followed by ionization through electron transfer from the analyte to DCTB cations. The electron transfer is thermochemically feasible, as the IE of phenanthrene (IE = 7.9 eV)[21] is 0.64 eV lower than the one of DCTB. Increasing the matrix-to-analyte ratio results overall in more efficient desorption and ionization of the analyte. Although in both positive-ion MALDI experiments, the molecular ion of DCTB is the most abundant matrix-derived ion, several matrix fragment ions[7] are also observed, which in principle could also participate in electron transfer with the analyte. Unfortunately, structures

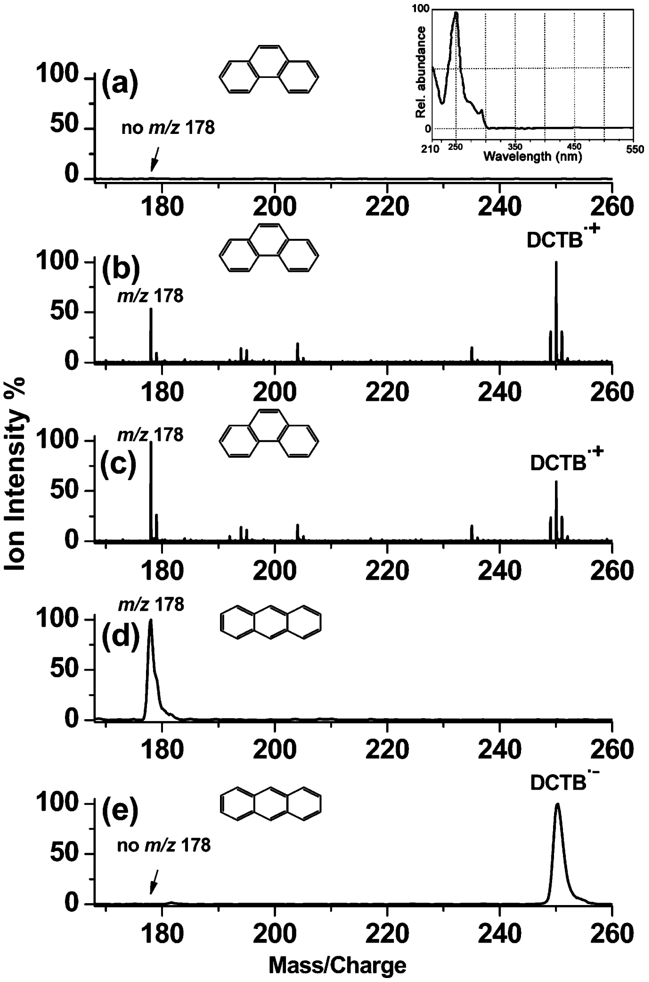

Figure 4. (a) Positive-ion (+) LDI of phenanthrene (inset: UV absorption of phenanthrene), (b) (+)-DCTB-MALDI of phenanthrene in a 1:1 matrix-to-analyte ratio, (c) (+)-DCTB-MALDI of phenanthrene in a 10:1 matrix-to-analyte ratio, (d) negative-ion (−) LDI of anthracene, and (e) (−)-DCTB-MALDI of anthracene in a 10:1 matrix-to-analyte ratio.

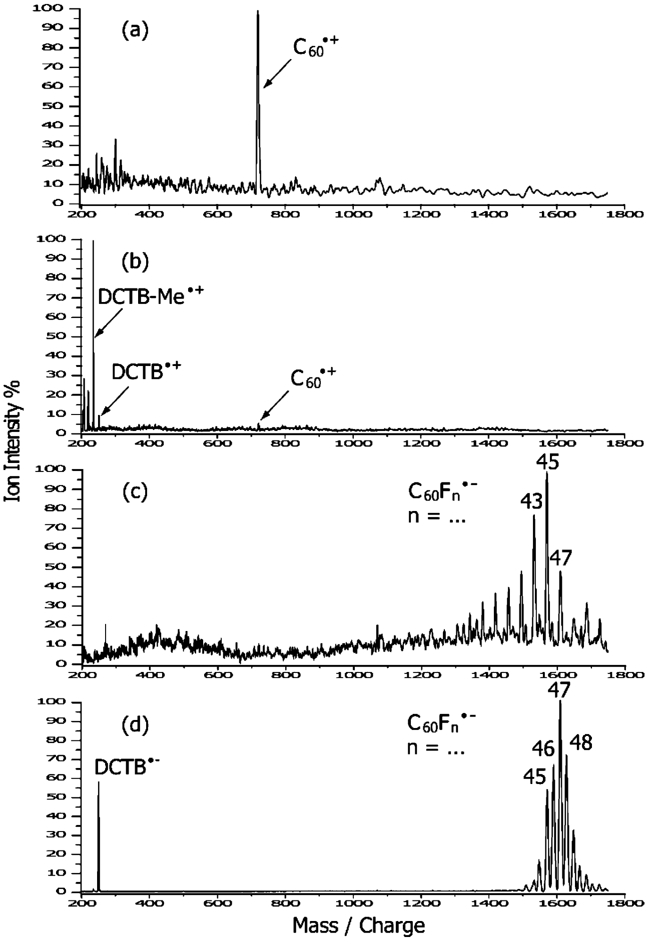

Figure 5. (a) Positive-ion (+) LDI of $C_{60}F_{46/48}$, (b) (+)-DCTB-MALDI of $C_{60}F_{46/48}$ in a 1000:1 matrix-to-analyte ratio, (c) negative-ion (−) LDI of $C_{60}F_{46/48}$, and (d) (−)-DCTB-MALDI of $C_{60}F_{46/48}$ in a 1000:1 matrix-to-analyte ratio.

and ionization energies of these ions are not available to allow further considerations.

Phenanthrene is not appropriate to monitor the electron-transfer reactivity in the negative-ion mode. Despite its suggested positive EA (EA_{phen} of approximately 0.3 eV)[22], earlier efforts failed to produce long-lived negative molecular ions of this compound by free electron attachment.[23] As a result, the fact that no negative molecular ions were observed in the present study by both direct LDI and MALDI resulted most likely from the fact that phenanthrene does not produce long-lived negative molecular ions. Therefore, isomeric anthracene was chosen as the model analyte for the negative-ion mode. Anthracene absorbs radiation at 337 nm and should be efficiently desorbed into the gas phase. In fact, direct LDI produces positively charged molecular ions abundantly, which have been used in related experiments to establish that electron transfer can constitute a means of forming analyte ions in MALDI.[24,25] In contrast to phenanthrene, the anthracene molecule produces long-lived molecular ions by free electron attachment[23] and possesses a larger EA ($EA_{anth} = 530 \pm 5$ meV).[26] Consequently, anthracene should produce negative molecular ions in direct LDI through free electron attachment but should fail to do so in DCTB-MALDI through electron transfer from $DCTB^{-\bullet}$ which is thermochemically unfavorable ($EA_{DCTB} = 2.0-2.3$ eV). These considerations are confirmed by Figures 4d,e, which represent the negative-ion direct LDI and DCTB-MALDI spectra of anthracene, respectively. The signals in Figures 4d,e are broader than those in Figures 4a−c because of the lower resolving power of the instrument used for these experiments (see Experimental Section). Direct LDI of anthracene leads to the formation of negative molecular ions (Figure 4d), which are entirely absent in DCTB-MALDI (Figure 4e, anthracene:DCTB ratio = 1:10) whereas the negative molecular ion of DCTB dominates the spectrum.

The fluorofullerene (FF) analytes, $C_{60}F_{46,48,}$ should feature the opposite electron-transfer reactivity with DCTB in MALDI. The high IE (12 eV)[27,28] prevents the formation of positive analyte ions through electron transfer to the $DCTB^{+\bullet}$ cation radical ($IE_{DCTB} = 8.54$ eV). Whereas the EA of 4.06 ± 0.25 eV [29] would allow the formation of negatively charged analyte ions by electron transfer from the $DCTB^{-\bullet}$ ($EA_{DCTB} = 2.0-2.3$ eV) molecular anion. Figure 5 compares the formation of FF ions of both polarities by direct LDI (Figure 5a positive and Figure 5c negative ion mode) and by DCTB-MALDI (Figure 5b positive and Figure 5d negative ion mode). Like phenanthrene, $C_{60}F_{46/48}$ is not absorbing at 337 nm.[30] However, direct LDI produces fragment ions derived from $C_{60}F_{46/48}$ in both ion modes. Because the formation of such ions is only observed at elevated laser fluences, we assume that nonresonant multiphoton absorption may play a substantial role. In positive-ion direct LDI (Figure 5a), the ionization of the FF sample would afford the accumulation of at least four photons to reach the IE = 12 eV with a photon energy of 3.68 eV at 337 nm.

Upon laser activation, F_2 loss becomes energetically more feasible than reaching the ionization threshold, so that F_2 loss prevails until C_{60} is formed. C_{60} shows a considerable resilience toward fragmentation (kinetic shift),[31] which may lead to the accumulation of energy well beyond the C_2-loss fragmentation barrier. Ionization can now successfully compete with fragmentation and the $C_{60}^{+\bullet}$ cation radical is observed. The $C_{60}^{+\bullet}$ ion observed in MALDI (Figure 5b), has probably the same mechanistic origin as in the direct LDI experiment, through the activation of FF sample that was not efficiently covered by the matrix. In line with the above thermochemical considerations, DCTB-MALDI fails to produce $C_{60}F_{46/48}^{+\bullet}$ cation radicals. Evidence of the sufficient desorption of neutral FFs into the gas phase is provided by the negative-ion spectra; one may therefore conclude that the positive ion formation was prevented purely on thermochemical grounds. The negative-ion direct LDI spectrum in Figure 5c shows the formation of FF ions with only uneven fluorine content. These ions are formed in the gas phase by attachment of free electrons that were released from the support by laser ablation. The attachment of energized electrons is dissociative, whereby the molecular anion may decompose through $F^\bullet$ loss into the more stable, even-electron anions of uneven fluorine content.[28] The resulting anions may dissociate further through the loss of F_2.[32]

In MALDI (Figure 5d) the more abundant DCTB matrix attracts the electrons in competition to the FF analyte. The electron transfer between the DCTB anion ($EA_{DCTB} = 2.0-2.3$ eV) and the FF ($EA_{C60F46/48} = 4.06 \pm 0.25$ eV) is now less exothermic than the free electron attachment to the FF. The free electron attachment would lead to $C_{60}F_{46/48}$ anions with internal excess energies in the range of 4 eV and because the loss of $F^\bullet$ from $C_{60}F_{48}^{-\bullet}$ affords only 2 eV,[11] dissociation is expected to prevail. Dissociative free electron attachment with loss of a fluorine atom has been observed, however, only at 4 eV, i.e., at an internal energy of the parent anion exceeding 8 eV.[28] In MALDI, the electron-transfer reaction between $DCTB^{-\cdot}$ and $C_{60}F_{48}$ is exothermic by only 2.1−1.8 eV, which is not markedly exceeding the energy requirement for further dissociations of the $C_{60}F_{48}^{-\bullet}$ anion.[11] The simultaneous formation of odd fluorine numbered anions (Figure 5d) is probably associated with thermal activation of the neutral species in the plume prior to the electron transfer with DCTB. In contrast to LDI, free electron attachment is in MALDI less likely to be pronounced, as the combination of the strong permanent accelerating voltage and the activation of a thick sample layer is known to diminish the free electron yield.[17]

In summary, the experimental findings are in excellent agreement with the assumption that DCTB-MALDI is governed by electron transfer reactions between matrix ions and analyte. Electron transfer is only observed when feasible within the thermochemical boundaries which are set by the IE and EA of DCTB and the analytes under study.

Conclusion

The IE of DCTB has been determined by PE spectroscopy as $IE_{vert} = 8.54 \pm 0.05$ eV and AM1 calculations lead to a value of 8.47 eV. The same level of theory predicts the electron affinity as EA = 2.3 eV, which agrees reasonably well with a recent DFT estimation of EA = 2 eV. In MALDI experiments using DCTB as the matrix and analytes of known thermochemistry, electron-transfer involving DCTB ions is not observed in reactions with analytes for which ionization would exceed thermochemical boundaries.

Acknowledgment. A.V.S. acknowledges INTAS for a Young Scientist Fellowship (No. 03-55-1811) supporting his work at Warwick. S.G.K. acknowledges the University of Warwick for a fully funded studentship. Financial support by the EPSRC (EP/C007999/1) for the establishment of a MALDI ToF/ToF instrument at Warwick is gratefully acknowledged.

References and Notes

(1) Frankevich, V. E.; Dashtiev, M.; Zenobi, R.; Kitagawa, T.; Lee, Y.; Murata, Y.; Yamazaki, T.; Gao, Y.; Komatsu, K.; Oliva, J. M. *Phys. Chem. Chem. Phys.* **2005**, *7*, 1036.

(2) Murata, Y.; Murata, M.; Komatsu, K. *J. Am. Chem. Soc.* **2003**, *125*, 7152.

(3) Vasil'ev, Y.; Wallis, D.; Drewello, T.; Nüchter, M.; Ondruschka, B.; Lobach, A. *Chem. Commun.* **2000**, 1233.

(4) Taylor, R.; Barrow, M. P.; Drewello, T. *Chem. Commun.* **1998**, 2497.

(5) Osterodt, J. V., Fritz. *Chem. Commun.* **1996**, 547.

(6) Lebedkin, S.; Ballenweg, S.; Gross, J.; Taylor, R.; Krätschmer, W. *Tetrahedron Lett.* **1995**, *36*, 4971.

(7) Ulmer, L.; Mattay, J.; Torres-Garcia, H. G.; Luftmann, H. *Eur. J. Mass Spectrom.* **2000**, *6* (1), 49−52.

(8) Brown, T.; Clipston, N. L.; Simjee, N.; Luftmann, H.; Hungerbühler, H.; Drewello, T. *Int. J. Mass Spectrom.* **2001**, *210*/*211* (1−3), 249−263.

(9) Fati, D.; Vasil'ev, Y. V.; Wachter, N. K.; Taylor, R.; Drewello, T. *Int. J. Mass Spectrom.* **2003**, *229*, 3.

(10) Fati, D.; Leeman, V.; Vasil'ev, Y. V.; Drewello, T. *J. Am. Soc. Mass Spectrom.* **2002**, *13*, 1448.

(11) Streletskii, A. V.; Ioffe, I. N.; Kotsiris, S. G.; Barrow, M. P.; Drewello, T.; Strauss, S. H.; Boltalina, O. V. *J. Phys. Chem. A* **2005**, *109*, 714.

(12) Vasil'ev, Y. V.; Kotsiris, S. G.; Bashkin, I. O.; Antonov, V. E.; Moravsky, A. P.; Drewello, T. *J. Phys. Chem. B* **2005**, *109*, 11875.

(13) Kuvychko, I. V.; Streletskii, A. V.; Popov, A. A.; Kotsiris, S. G.; Drewello, T.; Strauss, S. H.; Boltalina, O. V. *Chem. Eur. J.* **2005**, *11*, 5426.

(14) Meier, M. A. R.; Schubert, U. S. *Rev. Sci. Insrum.* **2005**, *76*, 062211.

(15) Wyatt, M. F.; Stein, B. K.; Brenton, A. G. *Anal. Chem.* **2006**, *78*, 199.

(16) Zenobi, R.; Knochenmuss, R. *Mass Spectrom. Rev.* **1999**, *17*, 337.

(17) Knochenmuss, R.; Zenobi, R. *Chem. Rev.* **2003**, *103*, 441.

(18) Zykov, B. G.; Martin, V. V.; Grigoryev, I. A. *J. Electron Spectrosc. Relat. Phenom.* **1991**, *56*, 73.

(19) Khvostenko, O. G.; Tzeplin, E. E.; Lomakin, G. S. *Chem. Phys. Lett.* **2002**, *355*, 457.

(20) Frisch, M. J.; Trucks, G. W.; Schlegel, H. B.; Scuseria, G. E.; Robb, M. A.; Cheeseman, J. R.; Zakrzewski, V. G.; Montgomery, J. A., Jr.; Stratmann, R. E.; Burant, J. C.; Dapprich, S.; Millam, J. M.; Daniels, A. D.; Kudin, K. N.; Strain, M. C.; Farkas, O.; Tomasi, J.; Barone, V.; Cossi, M.; Cammi, R.; Mennucci, B.; Pomelli, C.; Adamo, C.; Clifford, S.; Ochterski, J.; Petersson, G. A.; Ayala, P. Y.; Cui, Q.; Morokuma, K.; Malick, D. K.; Rabuck, A. D.; Raghavachari, K.; Foresman, J. B.; Cioslowski, J.; Ortiz, J. V.; Baboul, A. G.; Stefanov, B. B.; Liu, G.; Liashenko, A.; Piskorz, P.; Komaromi, I.; Gomperts, R.; Martin, R. L.; Fox, D. J.; Keith, T.; Al-Laham, M. A.; Peng, C. Y.; Nanayakkara, A.; Gonzalez, C.; Challacombe, M.; Gill, P. M. W.; Johnson, B.; Chen, W.; Wong, M. W.; Andres, J. L.; Gonzalez, C.; Head-Gordon, M.; Replogle, E. S.; Pople, J. A. Gaussian Inc., Pittsburgh, PA, 1998.

(21) Lias, S. G. Ionization Energy Evaluation. In *NIST Chemistry WebBook, NIST Standard Reference Database Number 69*; Linstrom, P. J., Mallard, W. G., Eds.; National Institute of Standards and Technology: Gaithersburg MD, 20899 (http://webbook.nist.gov), June 2005.

(22) Bartmess, J. E. Ionization Energy Evaluation. In *NIST Chemistry WebBook, NIST Standard Reference Database Number 69*; Linstrom, P. J., Mallard, W. G., Eds.; National Institute of Stanards and Technology: Gaithersburg MD, 20899 (http://webbook.nist.gov), June 2005.

(23) Tobita, S.; Meinke, M.; Illenberger, E.; Christophorou, L. G.; Baumgärtel, H.; Leach, S. *Chem. Phys.* **1992**, *161*, 501.

(24) McCarley, T. D.; McCarley, R. L.; Limbach, P. A. *Anal. Chem.* **1998**, *70*, 4376.

(25) Macha, S. F.; McCarley, T. D.; Limbach, P. A. *Anal. Chim. Acta* **1999**, *397*, 235.

(26) Schiedt, J.; Weinkauf, R. *Chem. Phys. Lett.* **1997**, *266*, 201.

(27) Steger, H.; Mische, U.; Kamke, W.; Ding, A.; Fieber-Erdmann, M.; Drewello, T. *Chem. Phys. Lett.* **1997**, *276*, 39.

(28) Vasil'ev, Y. U.; Boltalina, O. V.; Tuktarov, R. F.; Mazunov, V. A.; Sidorov, L. N. *Int. J. Mass Spectrom. Ion Processes* **1998**, *173*, 113.

(29) Hettich, R.; Jin, C. M.; Compton, R. *Int. J. Mass Spectrom. Ion Processes* **1994**, *138*, 263.

(30) Amarantov, S. V.; Bezmelnitsyn, V. N.; Boltalina, O. V.; Danailov, M.; Dudin, P. V.; Ryzkov, A. V.; Stankevitch, V. G. *Nuc. Inst. Methods Phys. Res. A* **2001**, *470*, 318.

(31) Lifshitz, C. *Eur. J. Mass Spectrom.* **2002**, *8*, 85.

(32) Cozzolino, R.; Belgacem, O.; Drewello, T.; Käseberg, L.; Herzschuh, R.; Suslov, S.; Boltalina, O. V. *Eur. Mass Spectrom.* **1997**, *3*, 407.